Chemistry & Biology
Article

Regulation of Telomere Length by G-Quadruplex Telomere DNA- and TERRA-Binding Protein TLS/FUS

Kentaro Takahama,[1] Asami Takada,[1] Shota Tada,[1] Mai Shimizu,[1] Kazutoshi Sayama,[2] Riki Kurokawa,[3] and Takanori Oyoshi[1,*]
[1]Faculty of Science, Department of Chemistry
[2]Faculty of Agriculture, Department of Applied Biological Chemistry
Shizuoka University, 836 Ohya Suruga, Shizuoka 422-8529, Japan
[3]Division of Gene Structure and Function, Saitama Medical University Research Center for Genomic Medicine, 1397-1 Yamane Hidaka, Saitama 350-1241, Japan
*Correspondence: stohyos@ipc.shizuoka.ac.jp
http://dx.doi.org/10.1016/j.chembiol.2013.02.013

SUMMARY

Mammalian telomeres comprise noncoding TTAGGG repeats in double-stranded regions with a single-stranded TTAGGG repeat 3′ overhang and are bound by a multiprotein complex with a telomeric repeat-containing RNA (TERRA) containing a UUAGGG repeat as a G-quadruplex noncoding RNA. TLS/FUS is a human telomere-binding protein that was first identified as an oncogenic fusion protein in human myxoid and round-cell liposarcoma. Here, we show that the Arg-Gly-Gly domain in the C-terminal region of TLS forms a ternary complex with human telomere G-quadruplex DNA and TERRA in vitro. Furthermore, TLS binds to G-quadruplex telomere DNA in double-stranded regions and to G-quadruplex TERRA, which regulates histone modifications of telomeres and telomere length in vivo. Our findings suggest that the G-quadruplex functions as a scaffold for the telomere-binding protein, TLS, to regulate telomere length by histone modifications.

INTRODUCTION

G-quadruplexes in the human genome are thought to have important biologic roles because they are found within the telomere, the physical end of eukaryotic chromosomes, and are associated with the promoters of several proto-oncogenes (Luu et al., 2006; Phan et al., 2004, 2007; Siddiqui-Jain et al., 2002). Human telomeres (Htelos) comprise TTAGGG repeats with a single-stranded G-rich 3′ overhang that forms an equilibrium G-quadruplex of the hybrid (3 + 1) form together with the parallel-stranded form and the basket-type antiparallel form in K^+ ion-containing solution and acts as a tumor suppressor by inhibiting telomerase (Lim et al., 2009; Luu et al., 2006; Singh et al., 2009; Zahler et al., 1991; Zaug et al., 2005). A recent analysis identified telomeric repeat-containing RNA (TERRA) as a component of telomeric heterochromatin, which contains tandem arrays of short RNA repeats r(UUAGGG) with variable subtelomeric sequences, that exists as a G-quadruplex formation of the parallel-stranded form in K^+ ion-containing solution and in vivo (Azzalin et al., 2007; Deng et al., 2009; Luke and Lingner, 2009; Martadinata and Phan, 2009; Schoeftner and Blasco, 2008; Xu et al., 2010). The functions of the G-quadruplex structures in telomere maintenance in human cells, however, are not clear because little is known about G-quadruplex-specific-binding proteins in Htelos. Telomere end-binding protein β-regulated G-quadruplex formation of a single-stranded telomere DNA in the protozoan ciliate *Stylonychia lemnae* and the yeast telomerase subunit Est1p promote the formation of a single-stranded telomere DNA to a G-quadruplex structure that is involved in maintaining telomere length (Paeschke et al., 2005; Zhang et al., 2010).

We previously reported that Ewing's sarcoma (EWS) binds to G-quadruplex-formed Htelo and TERRA and stabilizes the G-quadruplex Htelo formed by the RGG3 domain of EWS (Takahama et al., 2011a, 2011b). Based on the purification of human telomeric chromatin using proteomics of isolated chromatin segments, Déjardin and Kingston recently reported that "translocated in liposarcoma" (TLS) protein, also termed FUS, which is related to EWS as a subgroup within the RNP family of RNA-binding proteins, binds telomeres (Déjardin and Kingston, 2009). TLS was first identified in human myxoid and round-cell liposarcoma as an oncogenic fusion protein with a stress-induced DNA-binding transcription factor, CHOP (Crozat et al., 1993; Ron, 1997). In contrast to the clear understanding of TLS as a multifunctional protein responsible for a variety of regulatory processes, including transcription, mRNA splicing, and mRNA transport from the nucleus to the cytoplasm, the function and nucleic acid-binding properties of TLS on telomeres remain poorly characterized (Kanai et al., 2004; Yang et al., 1998; Yoshimura et al., 2006; Wang et al., 2008). Here, we show that the C-terminal (C term) Arg-Gly-Gly (RGG) domain in TLS specifically targets a fold in the G-quadruplex Htelo and TERRA and forms a ternary complex with these G-quadruplexes in vitro. Moreover, TLS binds G-quadruplex DNA in the telomere double-stranded region and G-quadruplex TERRA in vivo. Finally, overexpression of recombinant TLS results in heterochromatin and a shortening of the telomeres in vivo. Our findings suggest that the G-quadruplex in the telomere functions as

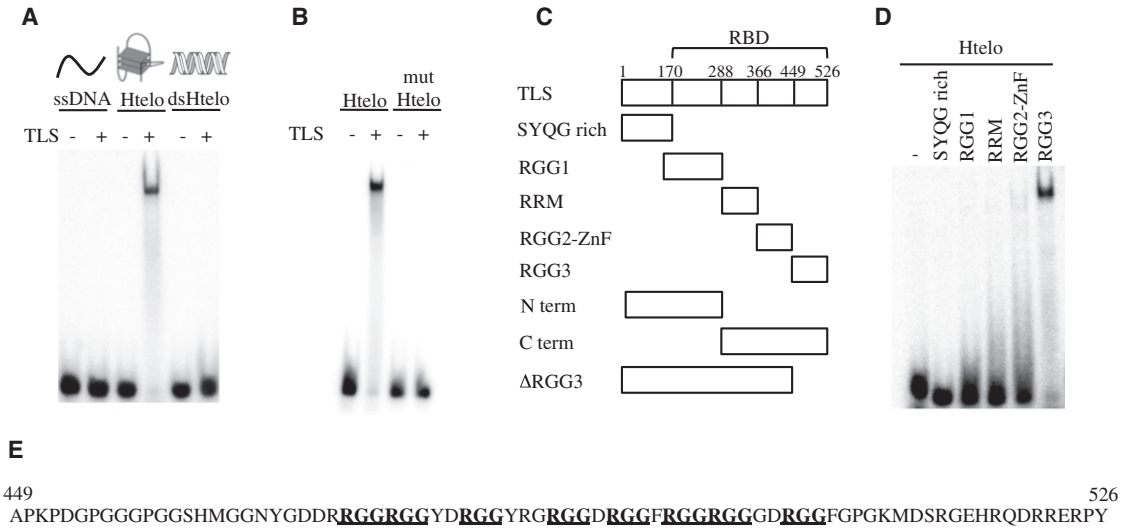

Figure 1. G-Quadruplex Telomere DNA Binding of TLS

(A) EMSA was performed with TLS and ssDNA, Htelo, or dsHtelo.

(B) EMSA was performed with TLS and either Htelo or mut Htelo.

(C) Schematic representation of the TLS mutants constructed to map the Htelo-binding specificity of each region of TLS: SYQG rich, Arg-Gly-Gly-rich motif 1 (RGG1), RNA recognition motif (RRM), Arg-Gly-Gly-rich motif 2 (RGG2), zinc finger (ZnF), Arg-Gly-Gly-rich motif 3 (RGG3), N terminal (N term), C terminal (C term), and TLS without RGG3 (ΔRGG3).

(D) Htelo-binding activities of the TLS mutants. EMSA was performed with these proteins and ^{32}P-labeled Htelo.

(E) Amino acid sequences of RGG3 are described. RGG motifs are underlined.

See also Figures S1–S3.

a scaffold for telomere-binding proteins to regulate telomere histone modifications and telomere length.

RESULTS

The RGG3 Region of TLS Binds with High Affinity to G-Quadruplex Htelo DNA

To investigate the ability of TLS to bind telomere DNA, an electrophoretic mobility shift assay (EMSA) of TLS was performed using a ^{32}P-labeled Htelo short repeat DNA d[AGGG(TTAGGG)$_3$] (Htelo) that exists as a G-quadruplex formation of the hybrid (3 + 1) form in K^+ ion-containing solution (Luu et al., 2006), the control single-stranded DNA (ssDNA), and Htelo duplex DNA (dsHtelo; Figure 1A; Table 1). Binding analysis revealed that TLS binds to G-quadruplex-formed Htelo, but not ssDNA or dsHtelo, in the presence of K^+. To test whether TLS specifically binds to Htelo folded into a G-quadruplex, we analyzed the binding between TLS and a mutated Htelo DNA d[AGGG(TTAGTG)$_2$TTAGGG] (mut Htelo) in which T is replaced with G at positions 9 and 15 in Htelo, which destabilizes the G-quadruplex formation, as previously demonstrated by circular dichroism (CD) spectroscopy (Table 1) (Takahama et al., 2011a). TLS bound to the Htelo folded in a G-quadruplex, but not to mut Htelo (Figure 1B). To further confirm whether formation of the G-quadruplex is necessary for TLS binding, we assayed the binding of TLS with Htelo in the presence of LiCl. The results indicated that TLS binding to Htelo in the presence of Li^+, which did not form the G-quadruplex, was abolished (Figure S1A available online). Furthermore, competitive experiments performed in the presence of unlabeled competitor Htelo, dsHtelo, or mut Htelo showed that Htelo effectively competed for TLS binding to Htelo, whereas dsHtelo or mut Htelo had no effect, even at a 100-fold M excess (Figures S1B–S1D). Previous studies reported that analogs of the cationic porphyrin tetra-(N-methyl-4-pyridyl)porphine (TMPyP4) recognize the G-quadruplex Htelo and inhibit telomerase activity (Parkinson et al., 2007; Wheelhouse et al., 1998). Competitive experiments performed in the presence of TMPyP4 showed that TMPyP4 effectively competed for Htelo binding with TLS (Figure S1E). These findings suggest that TLS binds to G-quadruplex Htelo with structural specificity.

TLS contains the S, Y, Q, and G-rich domain (SYQG rich) in the N-terminal region and the RNA-binding domain (RBD) in the C term region as multiple domains involved in nucleic acid-protein interactions: an RNA recognition motif (RRM) flanked by two regions in RGG repeats and a C_2C_2 zinc finger (ZnF) with an RGG domain in the C term (Wang et al., 2008). We further investigated the region of TLS that contributes to Htelo-binding specificity by comparing the behavior of various mutant recombinant proteins, i.e., SYQG rich (residues 1–169), RGG1 (residues 159–287), RRM (residues 288–365), RGG2 ZnF (residues 366–448), and RGG3 (residues 449–526) (Figure 1E), with regard to Htelo (Figure 1C). EMSA showed that RGG3 interacted with Htelo, whereas the proteins containing SYQG rich, RGG1, RRM, and RGG2 ZnF did not bind to Htelo (Figure 1D). To elucidate the binding ability of RGG3 to the G-quadruplex-formed Htelo, various concentrations of RGG3 were incubated with 5′ ^{32}P-labeled Htelo in K^+ solution (Figure S2A). The mobility shift data were fitted to a hyperbolic equation to give a K_D of 10 ± 2 nM. Competition experiments performed in the presence of TMPyP4 showed that TMPyP4 effectively competed for Htelo binding with RGG3 (Figure S1F). These findings suggest that

Table 1. Sequence of Oligonucleotides Used in EMSA and CD Spectroscopy

Name	Sequence
ssDNA	d(CATTCCCACCGGGACCACCAC)
Htelo	d[AGGG(TTAGGG)$_3$]
dsHtelo	d[AGGG(TTAGGG)$_3$]/d[(CCCTAA)$_3$CCCT]
mut Htelo	d[AGGG(TTAGTG)$_2$TTAGGG]
TERRA	r(UUAGGG)$_4$
mut TERRA	r[UUAGGG(UUAGUG)$_2$UUAGGG]
Htelo-biotin	d[AGGG(TTAGGG)$_3$]-biotin

Oligonucleotides were diluted to 0.5 mM (base concentration) in 50 mM Tris-HCl (pH 7.5) in the presence of 100 mM KCl or 100 mM LiCl, as specified. Duplex annealing or quadruplex formation was performed by heating the samples to 95°C on a thermal heating block and cooling to 4°C at a rate of 2°C/min.

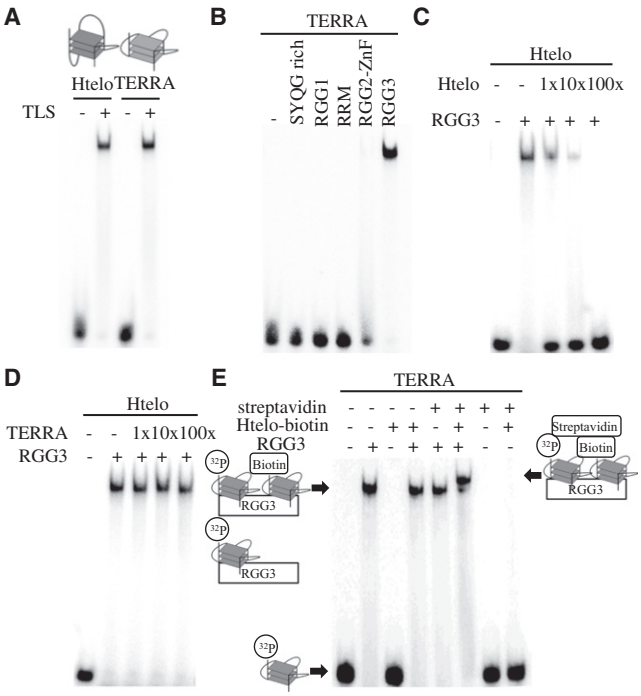

Figure 2. G-Quadruplex Telomere DNA and TERRA Binding of RGG3 in TLS In Vitro

(A) EMSA was performed with TLS and Htelo or TERRA.

(B) TERRA-binding activities of the TLS mutants. EMSA was performed with these proteins and ^{32}P-labeled TERRA.

(C and D) Binding competition assay, assaying binding of RGG3 to ^{32}P-labeled Htelo in the presence of unlabeled Htelo or TERRA.

(E) EMSA of ^{32}P-labeled TERRA and biotinylated Htelo with RGG3 was performed by adding streptavidin. Labeled TERRA and RGG3 (lanes 2, 4, 5, and 6) were incubated with (lanes 3, 4, 6, and 8) or without (lanes 1, 2, 5, and 7) Htelo-biotin in the presence (lanes 5, 6, 7, and 8) or absence (lanes 1, 2, 3, and 4) of streptavidin.

See also Figures S1–S4.

RGG3 binds to G-quadruplex Htelo with structure specificity. To investigate whether TLS binding of RGG3 affected the stability of the G-quadruplex structure of Htelo, we performed a polymerase stop assay. This assay showed that the stopping site corresponded to the base located 3′ to the first guanine base involved in the G-quadruplex formation (Takahama et al., 2011a). As the RGG3 protein concentration increased, the full-length product decreased, and the stopping site product increased (Figure S3A). These results indicate that RGG3 stabilizes the folded G-quadruplex formation.

The hybrid (3 + 1) form of human telomeric G-quadruplex DNA in K^+ is converted to a stable parallel-stranded form in K^+-containing solution with 40% (w/v) PEG200 within 24 hr due to water depletion (Figure S3B) (Heddi and Phan, 2011; Miyoshi et al., 2006; Xue et al., 2007). On the other hand, we reported that the RGG3 of EWS binds to the Htelo G-quadruplex and changes the hybrid (3 + 1) form of Htelo within 1 hr (Takahama et al., 2011a). To understand the induction of the G-quadruplex formation in Htelo by RGG3 of TLS, we performed a CD spectroscopic analysis of Htelo in the presence of various amounts of RGG3 in 1 hr (Figure S3C). The CD spectrum of Htelo, a hybrid (3 + 1) form, showed a strong positive band at 290 nm and a negative band around 235 nm, whereas the addition of 1 ratio excess of RGG3 induced an increase in ellipticity and shifted the spectrum from a strong positive band to a band at 265 nm and a negative band around 240 nm. These results suggest that the CD spectrum of Htelo with RGG3 is characterized as the parallel-stranded form, consistent with the results of previous CD studies (Xu et al., 2006). These findings indicate that RGG3 of TLS binds to the Htelo G-quadruplex and changes the hybrid (3 + 1) form of Htelo. Moreover, these data provide a model showing the change from the hybrid (3 + 1) form to the parallel-stranded form with the association of RGG3.

RGG3 of TLS Binds to a Htelo and TERRA Simultaneously via a G-Quadruplex-Dependent Interaction

A recent analysis identified that TERRA contains tandem arrays of short RNA repeats r(UUAGGG) with variable subtelomeric sequences and forms an integral component of telomeric heterochromatin (Deng et al., 2009). In vitro binding analysis showed that TLS binds to TERRA r(UUAGGG)$_4$ as well as Htelo in the presence of K^+ (Figure 2A; Table 1). Previous studies indicated that r(UUAGGG)$_4$ in K^+-containing solution exists as a G-quadruplex formation of the parallel-stranded form (Martadinata and Phan, 2009). To test whether TLS specifically binds to TERRA folded into a G-quadruplex, we analyzed the binding of TLS with a mutated TERRA r[UUAGGG(UUAGUG)$_2$UUAGGG] (mut TERRA), that replaces G with U at positions 11 and 17 of TERRA, or an unfolded TERRA in the presence of Li^+, which destabilizes the G-quadruplex formation as confirmed by CD (Table 1) (Takahama et al., 2011a). Our findings indicated that TLS binds to the folded TERRA G-quadruplex, but not to unfolded TERRA (Figures S1G and S1H). Furthermore, competition experiments in the presence of unlabeled competitor TERRA showed that TERRA effectively competed for RGG3 binding, whereas mut Htelo had no effect, even at a 100-fold M excess (Figures S1I and S1J). Competitive experiments carried out in the presence of TMPyP4 showed that TMPyP4 effectively competed for TERRA binding with TLS (Figure S1K). These findings suggest that TLS binds to G-quadruplex TERRA with structural specificity.

To investigate the region of TLS that contributes to TERRA-binding specificity by comparing the behavior of various mutant

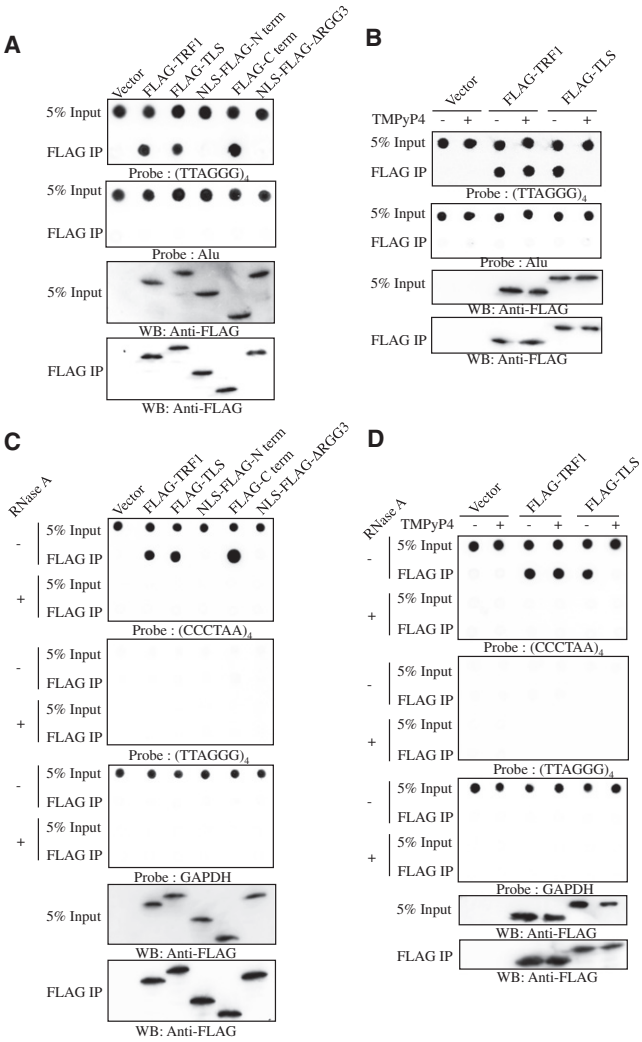

Figure 3. Telomere DNA and TERRA Binding of TLS In Vivo

(A) DNA ChIP assays were performed in HeLa S3 cells transfected with FLAG-TLS, NLS-FLAG-N term, FLAG-C term, NLS-FLAG-ΔRGG3, FLAG-TRF1, or expression vector alone. IP-recovered DNA was detected with probes $(TTAGGG)_4$ (top panel) or Alu (second panel). Five percent (5%) Input (third panel) and FLAG IP material (bottom panel) were detected by western blot (WB) with antibody to FLAG.

(B) Same as in (A), except transfection with FLAG-TLS, FLAG-TRF1, or expression vector alone incubated in the presence or absence of 100 μM TMPyP4 for 5 hr.

(C) RNA ChIP assays were performed in the same cells as in (A). ChIP RNA was either mock treated (−) or treated (+) with RNase A (200 μg/ml) prior to dot-blot analysis. RNA was visualized by hybridization with probes $(CCCTAA)_4$ (top panel), $(TTAGGG)_4$ (second panel), or GAPDH (third panel). Five percent (5%) Input (fourth panel) and FLAG IP material (bottom panel) were detected by western blot with antibody to FLAG.

(D) Same as in (C), except transfection with FLAG-TLS, FLAG-TRF1, or expression vector alone incubated in the presence or absence of TMPyP4. See also Figure S5.

recombinant proteins, we conducted EMSA of SYQG rich, RGG1, RRM, RGG2 ZnF, and RGG3 with Htelo (Figure 2B). EMSA showed that RGG3 strongly binds to TERRA, whereas proteins containing SYQG rich, RGG1, and RRM did not bind to it, and RGG2 ZnF weakly interacted with it. To elucidate the binding ability of RGG3 to the G-quadruplex TERRA, various concentrations of RGG3 were incubated with 5′ ^{32}P-labeled TERRA in K^+ solution (Figure S2B). The mobility shift data were fitted to a hyperbolic equation to give a K_D of 15 ± 2 nM. Competition experiments carried out in the presence of TMPyP4 showed that TMPyP4 effectively competed for TERRA binding with RGG3 (Figure S1L). These results indicate that RGG3 binds to G-quadruplex-formed TERRA. Moreover, incubation of TERRA with RGG3 did not alter the G-quadruplex RNA structures, as demonstrated by the CD spectrum analysis, even if a 1.2-fold excess of RGG3 was added (Figure S3D), indicating that RGG3 is unable to alter the parallel-stranded form of TERRA.

To investigate whether TERRA affects Htelo binding of RGG3, unlabeled TERRA or unlabeled Htelo was used in competition assays with ^{32}P-labeled Htelo to RGG3 (Figures 2C and 2D). Htelo binding of RGG3 was not affected by adding excess TERRA competitor, but it was affected by adding excess Htelo. Similarly, TERRA binding of RGG3 was not affected by adding excess Htelo competitor, but it was affected by adding excess TERRA (Figures S4A and S4B). We next developed an EMSA to investigate whether RGG3 binds to G-quadruplex Htelo and TERRA simultaneously. Using biotinylated Htelo and ^{32}P-labeled TERRA with RGG3 and streptavidin in an EMSA, streptavidin specificity promoted the formation of a supershifted product in the presence of RGG3, TERRA, and biotinylated Htelo (Figure 2E, lane 6; Table 1). Without the addition of streptavidin or biotinylated Htelo, mobility of the streptavidin-supershifted band was not observed (Figure 2E, lanes 4 and 5). These findings indicate that RGG3 forms a ternary complex with a G-quadruplex Htelo and TERRA. Moreover, using biotinylated Htelo and ^{32}P-labeled TERRA with TLS and streptavidin in an EMSA showed that streptavidin promoted the formation of a supershifted product (Figure S4C). These results suggested that full-length TLS forms a ternary complex with G-quadruplex Htelo and TERRA in vitro (Figure S4C).

TLS Binds to a Htelo in Telomere Double-Stranded Region and TERRA via a G-Quadruplex-Dependent Interaction In Vivo

To investigate whether telomere DNA binding of TLS is due to RGG3 in vivo, we performed a DNA chromatin immunoprecipitation (ChIP) assay with anti-FLAG antibodies to Flag-tagged TLS (FLAG-TLS) and the C term (residues 288–526; FLAG-C term), nuclear localization signal (NLS)-fused Flag-tagged N terminal (residues 1–287; NLS-FLAG-N term) and TLS-deleted RGG3 (residues 1–448; NLS-FLAG-ΔRGG3), and Flag-tagged TRF1 (FLAG-TRF1) in HeLa cells using a $(TTAGGG)_4$ probe that hybridizes to the telomere double-stranded region (Figure 3A). The N terminal and ΔRGG3, in which RGG3 as NLS is deleted, were fused to a NLS that functions to import proteins to the nucleus (Kino et al., 2011; Zinszner et al., 1997). The nuclear localization of TLS, NLS-N term, C term, and NLS-ΔRGG3 was confirmed by microscopy (Figure S5). FLAG-TRF1 was used as a positive control in the DNA ChIP assay because TRF1 is a telomere-binding and telomere maintenance-regulating protein (Blasco, 2007; Deng et al., 2009; de Lange, 2005). Each protein was expressed in HeLa cells and then analyzed by a DNA ChIP assay for telomere binding. To eliminate concerns of variations in antibody efficiency or accessibility and contamination of RNA, we

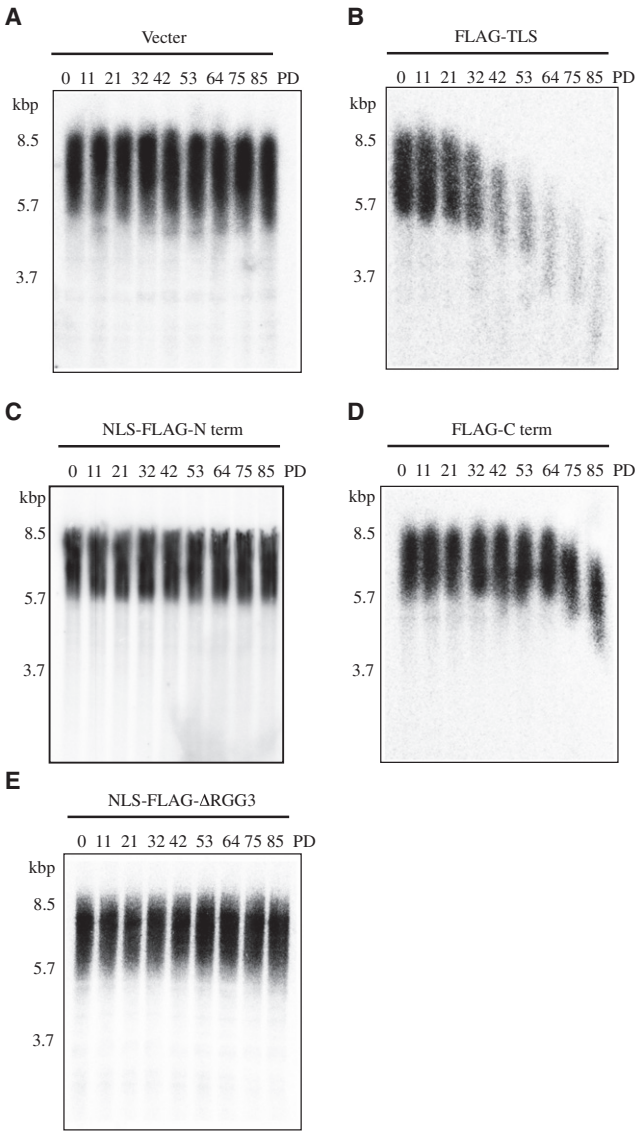

Figure 4. Telomere Length Changes in TLS- and C Term-overexpressed HeLa Cells

(A–E) Southern blots of HinfI/RsaI-digested genomic DNA from HeLa cell lines expressing FLAG-TLS (B), NLS-FLAG-N term (C), FLAG-C term (D), NLS-FLAG-ΔRGG3 (E), or expression vector alone (A). Each cell line was passaged for 85 population doublings (PD), and DNA samples were analyzed at the indicated PDs. Blots were probed with $(TTAGGG)_4$.

See also Figure S5.

used FLAG-tagged expression vectors and treated the samples with RNase A. The expression levels of input and immunoprecipitated protein by FLAG tag (FLAG IP) indicated that these proteins were recovered at similar levels by IP. FLAG-TLS and FLAG-C term, which include RGG3 in the C term region, as well as FLAG-TRF1 as a positive control, bound to telomere DNA, but not N-term and ΔRGG3. None of the DNA recovered from the FLAG IPs cross-reacted with Alu. These findings suggest that TLS interacts with the double-stranded region of the telomere through RGG3 in vivo. To identify whether TLS interacts with the G-quadruplex structure in telomere DNA in vivo, we performed DNA ChIP assays using a $(TTAGGG)_4$ probe with anti-FLAG antibodies in the presence or absence of TMPyP4 (Figure 3B). TMPyP4 inhibited telomere binding of TLS, but not TRF1, which is a double-stranded DNA-binding protein (Blasco, 2007; de Lange, 2005). These findings suggest that a G-quadruplex structure forms in the telomere double-stranded region, and TLS recognizes it with G-quadruplex structure specificity in vivo.

To identify whether TLS interacts with TERRA in vivo, i.e., a G-quadruplex structure (Xu et al., 2010), we performed RNA ChIP assays with anti-FLAG antibodies (Figure 3C). FLAG-TLS, NLS-FLAG-N term, FLAG-C term, and NLS-FLAG-ΔRGG3 were expressed in HeLa cells and then analyzed by RNA ChIP for TERRA binding. FLAG-TRF1 was used as a positive control because TRF1 binds TERRA (Deng et al., 2009). To avoid contamination of the DNA, we treated the samples with DNase I. FLAG-TLS and FLAG-C term, as well as FLAG-TRF1, bound to TERRA, but not NLS-FLAG-N term and NLS-FLAG-ΔRGG3. All of the RNA recovered from the FLAG was sensitive to RNase A and did not cross-react with GAPDH or $(TTAGGG)_4$ probes. The expression levels of input and IP protein indicated that all proteins were recovered at similar levels by IP. These findings suggest that TLS interacts with TERRA through RGG3 in vivo. To identify whether TLS interacts with the G-quadruplex structure in TERRA in vivo, we performed RNA ChIP assays with anti-FLAG antibodies in the presence or absence of TMPyP4 (Figure 3D). TMPyP4 inhibited TERRA binding of TLS, but not TRF1. These findings suggest that TLS specifically recognizes the G-quadruplex structure of TERRA in vivo (Figure 3).

Overexpression of Recombinant TLS Results in Telomere Shortening

Changes in the expression levels of TRF2, which influence the binding of the shelterin complex to double-stranded telomere DNA and have important roles in telomere structural maintenance, affect telomere length in mammalian cells (Karlseder et al., 2002; Wu et al., 2007). To test whether long-term overexpression of recombinant TLS affects telomere length in HeLa cells, we performed Southern blot analyses of HinfI and RsaI-digested genomic DNA from HeLa cells transfected with FLAG-TLS, NLS-FLAG-N term, FLAG-C term, NLS-FLAG-ΔRGG3, or expression vector alone (Figure 4). Each HeLa cell line transfected with NLS-FLAG-N term, NLS-FLAG-ΔRGG3, or expression vector alone had stable telomeres over 85 population doublings and with no effect on telomere length (Figures 4A, 4C, and 4E). In contrast, cells overexpressing FLAG-TLS showed gradual and progressive telomeric decline, and cells overexpressing FLAG-C term also showed gradual decline, but not to the degree of FLAG-TLS (Figures 4B and 4D). The loss of telomeric sequences was evident from the shortening of the terminal restriction fragments and from a reduction in the TTAGGG repeat signal. Expression of each recombinant TLS did not affect the cell viability or growth rate. These findings suggest the involvement of TLS in the RGG3-dependent regulation of telomere length (Figure 4).

Overexpression of Recombinant TLS Results in Histone Trimethylation of Telomeres

Telomere double-stranded DNA-binding protein TRF2 interacts with TERRA, which facilitates the trimethylation of histone H3

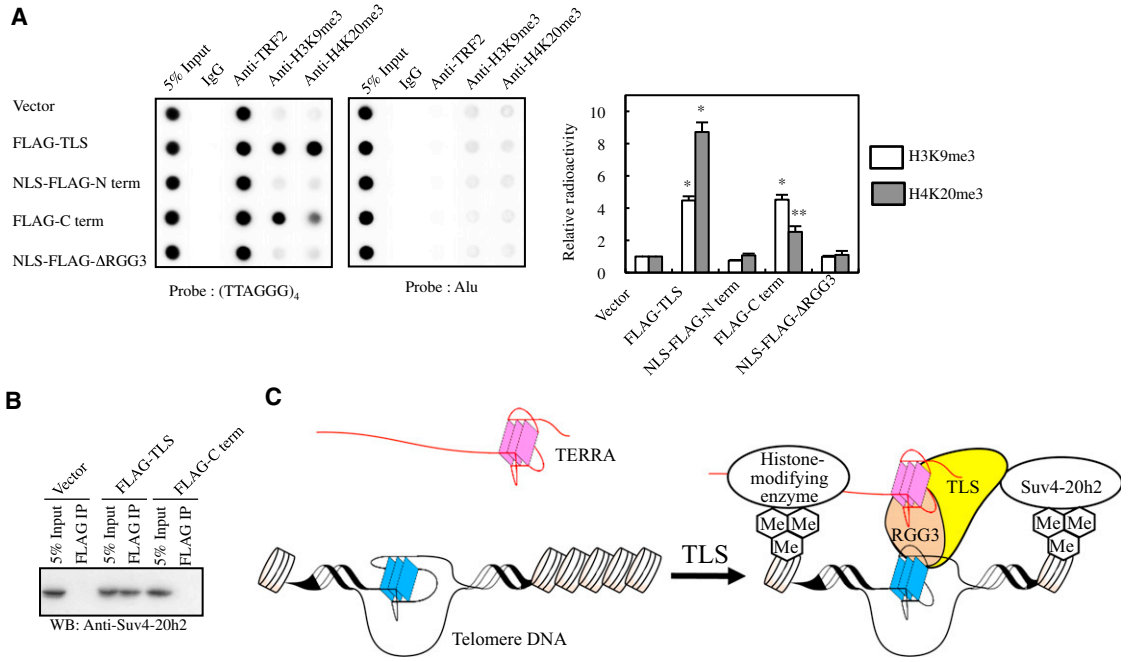

Figure 5. Histone Mark Changes in TLS- and C Term-Overexpressed HeLa Cells

(A) DNA ChIP assays were performed in the same cells (Figure 3A). Each IP-recovered DNA was visualized by hybridization with probes $(TTAGGG)_4$ (left) or Alu (middle). Antibodies specific for TRF2, H3K9me3, H4K20me3, or control IgG were used for the ChIP assays. The right panels show quantification of the ChIP assays represented by the left panels. Student's t test; *$p < 0.001$; **$p = 0.004$ compared with vector ($n = 4$). Bars represent mean values (± errors) obtained from four independent experiments.

(B) IP of FLAG-TLS or FLAG-C term with anti-FLAG antibody and detected by Suv4-20h2.

(C) Models of the proposed role of TLS in the telomere regions. Recruitment of Suv4-20h2 enzymes to the telomeres by TLS, which binds to G-quadruplex telomere DNA and TERRA depending on RGG3 region and the hybrid (3 + 1) form of Htelo changes to the parallel-stranded form with the association of RGG3, results in increasing H4K20 trimethylation and telomere shortening. The hypothetical mechanism of telomere shortening by H4K20 trimethylation is based on the previously reported role of Suv4-20h enzymes in telomere length control (Benetti et al., 2007b). The hypothesis of H3K9 trimethylation depending on TERRA binding to RGG3 of TLS is based on the previously reported model of histone-modifying enzymes with TERRA (Arnoult et al., 2012; Deng et al., 2009).

See also Figure S5.

at lysine 9 (H3K9me3) and origin recognition complex recruitment at telomeres, to maintain heterochromatin and DNA stability at telomeres (Deng et al., 2009). Moreover, the trimethylation of histone H4 at lysine 20 (H4K20me3) at telomeres induced by suppressor of variegation 4-20 homolog (Suv4-20h) histone methyltransferase contributes to control telomere length (Benetti et al., 2007b). To address whether the effects of TLS overexpression on telomere length were due to changes in histone modifications of telomeres, we performed DNA ChIP assays to detect H3K9me3 and H4K20me3 specifically at telomeric TTAGGG repeats in TLS- and TLS mutant-overexpressed cells (Figure 5A). Anti-TRF2 antibodies were used as a positive control in the DNA ChIP assay because TRF2 is a telomere-binding and telomere maintenance-regulating protein (Karlseder et al., 2002; Wu et al., 2007). DNA ChIP analysis with antibodies against H4K20me3 showed a progressive increase in the density of these histone modifications at telomeres in FLAG-TLS-overexpressed HeLa cells and only a small increase in FLAG-C term-overexpressed HeLa cells. On the other hand, DNA ChIP analysis with antibodies against H3K9me3 showed the same increase in the density of H3K9me3 modifications at telomeres in FLAG-TLS and FLAG-RBD-overexpressed HeLa cells. In HeLa cells transfected with NLS-FLAG-N term or NLS-FLAG-ΔRGG3, H3K9me3 and H4K20me3 modifications at the telomeres were not affected. As a control, the overexpressed TLS and other TLS mutant did not affect the histone modification at Alu. These findings suggested that H3K9me3 modification in telomeres is formed by C term, which binds to the G-quadruplex of TERRA and G-quadruplex DNA in the telomere double-stranded region, but the H4K20me3 modifications in telomeres are formed by full-length TLS, whereas the RGG3-deleted TLS, N term and ΔRGG3, do not promote the H3K20me3 and H4K20me3 modifications.

Suv4-20h2 is the main enzyme responsible for the H4K20me3 modification at telomeres, and abrogation of Suv4-20h2 histone methyltransferase results in telomere length deregulation (Benetti et al., 2007b). To determine whether TLS binds to Suv4-20h2, we tested whether TLS or RBD interacts with Suv4-20h2 in vivo using IP assays (Figure 5B). Nuclear extracts from HeLa cells transfected with FLAG-TLS, FLAG-C term, or expression vector alone were immunoprecipitated by anti-FLAG antibody and detected using an anti-Suv20h2 antibody. TLS bound to Suv4-20h2, but C term did not. Taken together, these findings suggested that full-length TLS directly interacts with Suv4-20h2, resulting in H4K20me3 modification at telomeres, whereas the C term of TLS does not (Figure 5C).

DISCUSSION

Here, we demonstrated that the RGG3 of the C term region in TLS binds to human telomeric DNA and TERRA with G-quadruplex structure specificity and forms a ternary complex with them in vitro (Figures 1 and 2). Previously, we reported that the arginine and aromatic residues of RGG3 in EWS are important for specific G-quadruplex binding (Takahama et al., 2011a, 2011b). In addition to RGG motif of RGG3 in EWS, the other arginine-rich regions of amino acids 639–656 (PGKMDKGEHRQERRDRPY) and proline-rich regions of amino acids 618–632 (PGGP PGPLMEQMGGR) are required for specific binding of G-quadruplex, too. Although RGG3, RGG2, and RGG1 in TLS are containing RGG repeats, phenylalanine, and tyrosine, only RGG3 in TLS has the homologous arginine-rich regions of amino acids 508–526 (PGKMDSRGEHRQDRRERPY) and proline-rich regions of amino acids 452–467 (PDGPGGGPGGSHMGGN) (Figure 1E). These findings may indicate that RGG3 in TLS recognizes specific G-quadruplex with similar binding mechanism of RGG3 in EWS.

Moreover, TLS bound to the G-quadruplex in the telomere double-stranded region and TERRA with G-quadruplex structure specificity, and histones in telomeres were modified by the overexpression of TLS or C term, resulting in in vivo telomere shortening (Figures 3–5). Previous studies demonstrated that Suv4-20h histone methyltransferases induce the trimethylation of H4K20 at telomeres (Benetti et al., 2007b). We showed H4K20me3 at telomeres in TLS-overexpressed cells and a direct interaction between TLS and Suv4-20h2 (Figure 5B), suggesting that TLS binds to the G-quadruplex as a scaffold in telomeres and has a role in controlling the H4K20me3 modification due to binding to Suv4-20h2 (Figure 5C). Trimethylation of H4K20 in FLAG-C term was slightly increased in overexpressed HeLa cells, although C term is not able to bind to Suv4-20h2, consistent with the findings from previous studies of the sequential induction of H3K9 and H4K20 trimethylation at heterochromatin (Benetti et al., 2007a; Schotta et al., 2004). Two main mechanisms of mammalian telomere maintenance have been described: the addition of telomeric repeats by telomerase, and an alternative mechanism that relies on recombination between telomeric sequences. A previous study suggested that Suv4-20h2-mediated H4K20me3 modifications in telomeres affect recombination (Benetti et al., 2007b). Therefore, TLS might regulate telomere length through telomere recombination due to H4K20me3 formed by Suv4-20h2. Previous studies suggested that stable G-quadruplex DNA comprised of TTAGGG repeats with a single-stranded G-rich 3′ overhang inhibits telomerase activity (Zahler et al., 1991; Zaug et al., 2005). A polymerase stop assay indicated that RGG3 of TLS stabilizes the folded G-quadruplex formation (Figure S3), but cells overexpressing C term showed only a small telomeric decline, whereas cells overexpressing TLS showed a progressive telomeric decline (Figure 4). This finding suggested that TLS does not regulate telomerase activity through G-quadruplex formation of the 3′ overhang but mainly alters telomere length through telomere recombination by promoting Suv4-20h2-mediated H4K20me3 modification.

On the other hand, TERRA associated with TRF1 and TRF2 is a component of mammalian telomeres, and the functions of TERRA suggest important roles in H3K9me3 modifications in telomeres (Arnoult et al., 2012; Deng et al., 2009). Recent studies reported that TERRA is associated with several heterochromatin marks, including the origin recognition complex, H3K9me3, and HP1 (heterochromatin protein 1) isoforms known to accumulate at constitutive heterochromatin (Deng et al., 2009). The origin recognition complex is also implicated in heterochromatin formation (Prasanth et al., 2004). In the present study, H3K9 in C term or TLS-overexpressed cells at telomeres was trimethylated (Figure 5A), suggesting that the C term in TLS acts as a link between TERRA and chromatin by forming a ternary complex with G-quadruplex telomere DNA and facilitates the H3K9me3 histone modification by associating with histone-modifying enzymes via TERRA (Figure 5C). Furthermore, the TERRA G-quadruplex is a common structural component of mammalian telomeres (Xu et al., 2010). In this paper, we demonstrated that TLS binds to TERRA with G-quadruplex specificity in vitro and in vivo. Recently, Balasubramanian et al. reported that TRF2 binds TERRA via interactions that require the formation of a G-quadruplex structure (Biffi et al., 2012). Telomere-binding proteins, such as TLS and TRF2, might promote the accumulation of TERRA and heterochromatin at the telomere via interactions with the TERRA G-quadruplex. Previously, a number of compounds that recognize the G-quadruplex in a single-stranded 3′ overhang of the telomere were developed as telomerase inhibitors (Ou et al., 2008). Therefore, G-quadruplex structures that not only comprise a single-stranded 3′ overhang but also a double-stranded telomere region are potential anticancer targets because the telomere is essential for genome integrity and plays an important role in cellular aging and cancer.

SIGNIFICANCE

G-quadruplexes in the human genome are thought to have important biologic roles because they are found within the telomere (Luu et al., 2006). Human telomeres comprise TTAGGG repeats with a single-stranded G-rich 3′ overhang that forms an equilibrium G-quadruplex in K^+ ion-containing solution (Lim et al., 2009; Luu et al., 2006; Singh et al., 2009). A recent analysis identified telomeric repeat-containing RNA (TERRA) as a component of telomeric heterochromatin, which contains tandem arrays of short RNA repeats r(UUAGGG) with variable subtelomeric sequences, that exists as a G-quadruplex formation of the parallel-stranded form in K^+ ion-containing solution (Azzalin et al., 2007; Martadinata and Phan, 2009; Xu et al., 2010). The functions of the G-quadruplex structures in telomere maintenance in human cells, however, are not clear because little is known about G-quadruplex-specific binding proteins in human telomeres. Here, we show that the Arg-Gly-Gly domain in the C term region of TLS forms a ternary complex with human telomere G-quadruplex DNA and TERRA in vitro. Furthermore, TLS binds to G-quadruplex telomere DNA in double-stranded regions and to G-quadruplex TERRA, which regulates histone modifications of telomeres and telomere length in vivo. Especially, DNA ChIP analysis with antibodies against the trimethylation of histone H4 at lysine 20 showed a progressive increase in the density of these histone modifications at telomeres in FLAG-TLS-overexpressed HeLa

cells. On the other hand, in HeLa cells transfected with TLS-deleted Arg-Gly-Gly domain, trimethylation of it at the telomeres was not affected. Our findings suggest that the G-quadruplex functions as a scaffold for the telomere-binding protein, TLS, to regulate telomere length by histone modifications.

EXPERIMENTAL PROCEDURES

Plasmid Constructs

The methods for producing the plasmid constructs and primer sets used for plasmid construction are described in the Supplemental Experimental Procedures. All DNA primers and other oligomers were obtained from Operon Biotechnologies (Tokyo), and all constructs were verified by automated DNA sequencing.

Expression and Purification of Glutathione S-Transferase Fusion Proteins

All recombinant proteins for in vitro experiments were fused to glutathione S-transferase (GST) at the N terminus and overexpressed in *Escherichia coli* as described previously (Takahama et al., 2011a, 2011b). The protein concentrations were determined using a BCA Protein Assay Kit (Thermo Scientific, Barrington, IL, USA).

EMSA

EMSAs were performed as described previously (Takahama et al., 2011a, 2011b). Samples of labeled oligonucleotides with each protein were incubated for 1 hr at 20°C and then loaded on a 6% polyacrylamide (acrylamide/bisacrylamide, 19:1) nondenaturing gel. All gels were exposed in a phosphorimager cassette and imaged (Personal Molecular Imager FX; Bio-Rad, Hercules, CA, USA).

EMSA with Streptavidin

Binding reactions were performed in a final volume of 20 μl using 20 fmol of the labeled oligonucleotide, which was folded by heating the samples to 95°C on a thermal heating block and cooling them to 4°C at a rate of 2°C/min, and 250 nM of purified RGG3 in a binding buffer (50 mM Tris-HCl [pH 7.5], 0.5 mM EDTA, 0.5 mM dithiothreitol, 0.1 mg/ml BSA, 1 μg/ml calf thymus DNA, and 100 mM KCl). After the samples were incubated with 100 nM streptavidin for 1 hr at 20°C, they were loaded onto an 8% polyacrylamide (acrylamide/bisacrylamide, 19:1) nondenaturing gel. TBE (0.5×) with 20 mM KCl was used, both in the gel and as the electrophoresis buffer. Electrophoresis was performed at 10 V/cm for 2 hr at 4°C, and the gels were visualized on a phosphorimager.

Cell Culture and Transfection

Cell culture and transfection were performed as described previously by Wang et al. (2008). HeLa cells were maintained in Dulbecco's modified Eagle's medium supplemented with 10% fetal bovine serum. For assays, cells were cultured in 6-well plates and transfected with plasmids for protein expression using Lipofectamine 2000 (Life Technologies, Carlsbad, CA, USA) according to the manufacturer's instructions. G418 (200 μg/ml) was added to the culture media every 3 days. HeLa cells were incubated in the presence or absence of 100 μM TMPyP4 for 5 hr and further analyzed using a DNA ChIP and RNA ChIP assay.

DNA ChIP Assay

The DNA ChIP assay was performed as described previously by Benetti et al. (2007a). HeLa cells infected with FLAG-TLS and FLAG-C term, or NLS-FLAG-N term and ΔRGG3 (NLS-FLAG-ΔRGG3), or control vector were crosslinked with 1% formaldehyde for 15 min at 25°C, and the crosslinking was stopped by the addition of 125 mM glycine. Cells were lysed and sonicated to obtain DNA fragments of 500–1,000 bp. For each IP, 1 μg of protein lysate with RNase A was used with 4 μg of mouse monoclonal anti-FLAG M2 antibody (Sigma-Aldrich, St. Louis), rabbit polyclonal anti-TRF2 antibody (Santa Cruz Biotechnology, Santa Cruz, CA, USA), rabbit polyclonal anti-trimethyl-histone H3 (Lys9) antibody (Millipore, Billerica, MA, USA), rabbit polyclonal anti-trimethyl-histone H4 (Lys20) antibody (Millipore), or normal mouse control IgG (Santa Cruz Biotechnology). The immunoprecipitated DNA was extracted and transferred to membranes (Immobilon; Millipore). Duplicate membranes were hybridized with a radioactive telomeric repeat probe $(TTAGGG)_4$ or an Alu repeat probe (CACGCC TGTAAT CCCAGC ACTTTG), and the gels were visualized on a phosphorimager.

RNA ChIP Assay

The RNA ChIP assay was performed as previously described by Deng et al. (2009). HeLa cells infected with FLAG-TLS, NLS-FLAG-N term, FLAG-C term, NLS-FLAG-ΔRGG3, and control vector were crosslinked with 1% formaldehyde for 15 min at 25°C, and the crosslinking was stopped by the addition of 125 mM glycine. For each IP, 1 μg of protein lysate with DNase I was used with 4 μg of mouse monoclonal anti-FLAG M2 antibody and Protein G-Agarose (Roche, Switzerland) at 4°C overnight and further analyzed using the method described above.

Western Blot Analysis

FLAG-TLS, NLS-FLAG-N term, FLAG-C term, and NLS-FLAG-ΔRGG3 were analyzed by SDS-PAGE in a 12% gel. Flag-tagged proteins were visualized by transferring to a polyvinylidene difluoride membrane and probed with a mouse monoclonal anti-FLAG M2 antibody. The secondary antibodies included anti-mouse horseradish peroxidase (Cell Signaling Technology, Danvers, MA, USA). Protein bands were visualized using the ECL western blotting analysis system (GE Healthcare, UK).

Telomeric Restriction Fragment Analysis

Telomeric restriction fragment analysis was performed as described previously by Counter et al. (1992) and Ludérus et al. (1996). The extracted RNA-free genomic DNA sample was digested with 25 U each of the HinfI and RsaI restriction enzymes at 37°C overnight and fractionated in a 0.7% agarose gel for 7 hr at 70 V. The gel was denatured/neutralized, and the DNA was transferred onto Hybond-N^+ membrane (GE Healthcare), crosslinked, and hybridized overnight with ^{32}P-end-labeled oligonucleotide $(TTAGGG)_4$. Gels were visualized on a phosphorimager.

IP and Western Blotting

Nuclear extracts from HeLa cells infected with FLAG-TLS, FLAG-C term, and control vector were prepared, and IP was conducted as previously described by Du et al. (2011) and Wang et al. (2008) using a mouse monoclonal anti-FLAG M2 antibody. SDS-PAGE and western blotting analysis were performed as described above, probing with rabbit polyclonal anti-FLAG antibody (Medical & Biological Laboratories, Nagoya, Japan) or anti-Suv4-20h2 (71–85) antibody (Sigma-Aldrich).

SUPPLEMENTAL INFORMATION

Supplemental Information includes five figures and Supplemental Experimental Procedures and can be found with this article online at http://dx.doi.org/10.1016/j.chembiol.2013.02.013.

ACKNOWLEDGMENTS

This research was supported by a Grant-in-Aid for Young Scientists (B) (No. 20750130 to T.O.) and a Grant-in-Aid for JSPS Fellows (No. 243925 to K.T.) from the Ministry of Education, Science, Sports, and Culture of Japan.

Received: December 5, 2012
Revised: February 19, 2013
Accepted: February 20, 2013
Published: March 21, 2013

REFERENCES

Arnoult, N., Van Beneden, A., and Decottignies, A. (2012). Telomere length regulates TERRA levels through increased trimethylation of telomeric H3K9 and HP1α. Nat. Struct. Mol. Biol. *19*, 948–956.

Azzalin, C.M., Reichenbach, P., Khoriauli, L., Giulotto, E., and Lingner, J. (2007). Telomeric repeat containing RNA and RNA surveillance factors at mammalian chromosome ends. Science *318*, 798–801.

Benetti, R., García-Cao, M., and Blasco, M.A. (2007a). Telomere length regulates the epigenetic status of mammalian telomeres and subtelomeres. Nat. Genet. *39*, 243–250.

Benetti, R., Gonzalo, S., Jaco, I., Schotta, G., Klatt, P., Jenuwein, T., and Blasco, M.A. (2007b). Suv4-20h deficiency results in telomere elongation and derepression of telomere recombination. J. Cell Biol. *178*, 925–936.

Biffi, G., Tannahill, D., and Balasubramanian, S. (2012). An intramolecular G-quadruplex structure is required for binding of telomeric repeat-containing RNA to the telomeric protein TRF2. J. Am. Chem. Soc. *134*, 11974–11976.

Blasco, M.A. (2007). The epigenetic regulation of mammalian telomeres. Nat. Rev. Genet. *8*, 299–309.

Counter, C.M., Avilion, A.A., LeFeuvre, C.E., Stewart, N.G., Greider, C.W., Harley, C.B., and Bacchetti, S. (1992). Telomere shortening associated with chromosome instability is arrested in immortal cells which express telomerase activity. EMBO J. *11*, 1921–1929.

Crozat, A., Aman, P., Mandahl, N., and Ron, D. (1993). Fusion of CHOP to a novel RNA-binding protein in human myxoid liposarcoma. Nature *363*, 640–644.

Déjardin, J., and Kingston, R.E. (2009). Purification of proteins associated with specific genomic Loci. Cell *136*, 175–186.

de Lange, T. (2005). Shelterin: the protein complex that shapes and safeguards human telomeres. Genes Dev. *19*, 2100–2110.

Deng, Z., Norseen, J., Wiedmer, A., Riethman, H., and Lieberman, P.M. (2009). TERRA RNA binding to TRF2 facilitates heterochromatin formation and ORC recruitment at telomeres. Mol. Cell *35*, 403–413.

Du, K., Arai, S., Kawamura, T., Matsushita, A., and Kurokawa, R. (2011). TLS and PRMT1 synergistically coactivate transcription at the survivin promoter through TLS arginine methylation. Biochem. Biophys. Res. Commun. *404*, 991–996.

Heddi, B., and Phan, A.T. (2011). Structure of human telomeric DNA in crowded solution. J. Am. Chem. Soc. *133*, 9824–9833.

Kanai, Y., Dohmae, N., and Hirokawa, N. (2004). Kinesin transports RNA: isolation and characterization of an RNA-transporting granule. Neuron *43*, 513–525.

Karlseder, J., Smogorzewska, A., and de Lange, T. (2002). Senescence induced by altered telomere state, not telomere loss. Science *295*, 2446–2449.

Kino, Y., Washizu, C., Aquilanti, E., Okuno, M., Kurosawa, M., Yamada, M., Doi, H., and Nukina, N. (2011). Intracellular localization and splicing regulation of FUS/TLS are variably affected by amyotrophic lateral sclerosis-linked mutations. Nucleic Acids Res. *39*, 2781–2798.

Lim, K.W., Amrane, S., Bouaziz, S., Xu, W., Mu, Y., Patel, D.J., Luu, K.N., and Phan, A.T. (2009). Structure of the human telomere in K^+ solution: a stable basket-type G-quadruplex with only two G-tetrad layers. J. Am. Chem. Soc. *131*, 4301–4309.

Ludérus, M.E., van Steensel, B., Chong, L., Sibon, O.C., Cremers, F.F., and de Lange, T. (1996). Structure, subnuclear distribution, and nuclear matrix association of the mammalian telomeric complex. J. Cell Biol. *135*, 867–881.

Luke, B., and Lingner, J. (2009). TERRA: telomeric repeat-containing RNA. EMBO J. *28*, 2503–2510.

Luu, K.N., Phan, A.T., Kuryavyi, V., Lacroix, L., and Patel, D.J. (2006). Structure of the human telomere in K+ solution: an intramolecular (3 + 1) G-quadruplex scaffold. J. Am. Chem. Soc. *128*, 9963–9970.

Martadinata, H., and Phan, A.T. (2009). Structure of propeller-type parallel-stranded RNA G-quadruplexes, formed by human telomeric RNA sequences in K^+ solution. J. Am. Chem. Soc. *131*, 2570–2578.

Miyoshi, D., Karimata, H., and Sugimoto, N. (2006). Hydration regulates thermodynamics of G-quadruplex formation under molecular crowding conditions. J. Am. Chem. Soc. *128*, 7957–7963.

Ou, T.M., Lu, Y.J., Tan, J.H., Huang, Z.S., Wong, K.Y., and Gu, L.Q. (2008). G-quadruplexes: targets in anticancer drug design. ChemMedChem *3*, 690–713.

Paeschke, K., Simonsson, T., Postberg, J., Rhodes, D., and Lipps, H.J. (2005). Telomere end-binding proteins control the formation of G-quadruplex DNA structures in vivo. Nat. Struct. Mol. Biol. *12*, 847–854.

Parkinson, G.N., Ghosh, R., and Neidle, S. (2007). Structural basis for binding of porphyrin to human telomeres. Biochemistry *46*, 2390–2397.

Phan, A.T., Modi, Y.S., and Patel, D.J. (2004). Propeller-type parallel-stranded G-quadruplexes in the human c-myc promoter. J. Am. Chem. Soc. *126*, 8710–8716.

Phan, A.T., Kuryavyi, V., Burge, S., Neidle, S., and Patel, D.J. (2007). Structure of an unprecedented G-quadruplex scaffold in the human c-kit promoter. J. Am. Chem. Soc. *129*, 4386–4392.

Prasanth, S.G., Prasanth, K.V., Siddiqui, K., Spector, D.L., and Stillman, B. (2004). Human Orc2 localizes to centrosomes, centromeres and heterochromatin during chromosome inheritance. EMBO J. *23*, 2651–2663.

Ron, D. (1997). TLS-CHOP and the role of RNA-binding proteins in oncogenic transformation. Curr. Top. Microbiol. Immunol. *220*, 131–142.

Schoeftner, S., and Blasco, M.A. (2008). Developmentally regulated transcription of mammalian telomeres by DNA-dependent RNA polymerase II. Nat. Cell Biol. *10*, 228–236.

Schotta, G., Lachner, M., Sarma, K., Ebert, A., Sengupta, R., Reuter, G., Reinberg, D., and Jenuwein, T. (2004). A silencing pathway to induce H3-K9 and H4-K20 trimethylation at constitutive heterochromatin. Genes Dev. *18*, 1251–1262.

Siddiqui-Jain, A., Grand, C.L., Bearss, D.J., and Hurley, L.H. (2002). Direct evidence for a G-quadruplex in a promoter region and its targeting with a small molecule to repress c-MYC transcription. Proc. Natl. Acad. Sci. USA *99*, 11593–11598.

Singh, V., Azarkh, M., Exner, T.E., Hartig, J.S., and Drescher, M. (2009). Human telomeric quadruplex conformations studies by pulsed EPR. Angew. Chem. Int. Ed. Engl. *48*, 9728–9730.

Takahama, K., Kino, K., Arai, S., Kurokawa, R., and Oyoshi, T. (2011a). Identification of Ewing's sarcoma protein as a G-quadruplex DNA- and RNA-binding protein. FEBS J. *278*, 988–998.

Takahama, K., Sugimoto, C., Arai, S., Kurokawa, R., and Oyoshi, T. (2011b). Loop lengths of G-quadruplex structures affect the G-quadruplex DNA binding selectivity of the RGG motif in Ewing's sarcoma. Biochemistry *50*, 5369–5378.

Wang, X., Arai, S., Song, X., Reichart, D., Du, K., Pascual, G., Tempst, P., Rosenfeld, M.G., Glass, C.K., and Kurokawa, R. (2008). Induced ncRNAs allosterically modify RNA-binding proteins in cis to inhibit transcription. Nature *454*, 126–130.

Wheelhouse, R.T., Sun, D., Han, H., Han, F.X., and Hurley, L.H. (1998). Cationic porphyrins as telomerase inhibitors: the interaction of tetra-(N-methyl-4-pyridyl)porphine with quadruplex DNA. J. Am. Chem. Soc. *120*, 3261–3262.

Wu, Y., Zacal, N.J., Rainbow, A.J., and Zhu, X.D. (2007). XPF with mutations in its conserved nuclease domain is defective in DNA repair but functions in TRF2-mediated telomere shortening. DNA Repair (Amst.) *6*, 157–166.

Xu, Y., Noguchi, Y., and Sugiyama, H. (2006). The new models of the human telomere d[AGGG(TTAGGG)3] in K+ solution. Bioorg. Med. Chem. *14*, 5584–5591.

Xu, Y., Suzuki, Y., Ito, K., and Komiyama, M. (2010). Telomeric repeat-containing RNA structure in living cells. Proc. Natl. Acad. Sci. USA *107*, 14579–14584.

Xue, Y., Kan, Z.Y., Wang, Q., Yao, Y., Liu, J., Hao, Y.H., and Tan, Z. (2007). Human telomeric DNA forms parallel-stranded intramolecular G-quadruplex in K+ solution under molecular crowding condition. J. Am. Chem. Soc. *129*, 11185–11191.

Yang, L., Embree, L.J., Tsai, S., and Hickstein, D.D. (1998). Oncoprotein TLS interacts with serine-arginine proteins involved in RNA splicing. J. Biol. Chem. *273*, 27761–27764.

Yoshimura, A., Fujii, R., Watanabe, Y., Okabe, S., Fukui, K., and Takumi, T. (2006). Myosin-Va facilitates the accumulation of mRNA/protein complex in dendritic spines. Curr. Biol. *16*, 2345–2351.

Zahler, A.M., Williamson, J.R., Cech, T.R., and Prescott, D.M. (1991). Inhibition of telomerase by G-quartet DNA structures. Nature *350*, 718–720.

Zaug, A.J., Podell, E.R., and Cech, T.R. (2005). Human POT1 disrupts telomeric G-quadruplexes allowing telomerase extension in vitro. Proc. Natl. Acad. Sci. USA *102*, 10864–10869.

Zhang, M.L., Tong, X.J., Fu, X.H., Zhou, B.O., Wang, J., Liao, X.H., Li, Q.J., Shen, N., Ding, J., and Zhou, J.Q. (2010). Yeast telomerase subunit Est1p has guanine quadruplex-promoting activity that is required for telomere elongation. Nat. Struct. Mol. Biol. *17*, 202–209.

Zinszner, H., Immanuel, D., Yin, Y., Liang, F.X., and Ron, D. (1997). A topogenic role for the oncogenic N-terminus of TLS: nucleolar localization when transcription is inhibited. Oncogene *14*, 451–461.

